

Electroluminescent properties of erbium-doped III–N light-emitting diodes

J. M. Zavada^{a)}

U.S. Army Research Office, Durham, North Carolina 27709

S. X. Jin, N. Nepal, J. Y. Lin, and H. X. Jiang

Department of Physics, Kansas State University, Manhattan, Kansas 66506

P. Chow and B. Hertog

SVT Associates, Incorporated, Eden Prairie, Minnesota 55344

(Received 9 September 2003; accepted 18 December 2003)

We report on the synthesis of Er-doped III–N double heterostructure light-emitting diodes (LEDs) and their electroluminescence (EL) properties. The device structures were grown through a combination of metalorganic chemical vapor deposition (MOCVD) and molecular-beam epitaxy (MBE) on *c*-plane sapphire substrates. The AlGaN layers, with an Al concentration of $\sim 12\%$, were prepared by MOCVD and doped with Si or Mg to achieve *n*- and *p*-type conductivity, respectively. The Er+O-doped GaN active region was grown by MBE and had a thickness of 50 nm. The Er concentration was estimated to be $\sim 10^{18} \text{ cm}^{-3}$. The multilayer *n*-AlGaN/GaN:Er/*p*-AlGaN structures were processed into LEDs using standard etching and contacting methods. Several different LEDs were produced and EL spectra were recorded with both forward and reverse bias conditions. Typically, the EL under reverse bias was five to ten times more intense than that under forward bias. The LEDs displayed a number of narrow emission lines representative of the GaN:Er system (green: 539 nm, 559 nm; infrared: 1000 nm, 1530 nm). While some current crowding was observed, green emission was visible under ambient room conditions at 300 K. At cryogenic temperatures, the emission lines increased in intensity and had a narrower linewidth. EL spectra were recorded down to 10 K and the L-I characteristics were systematically measured. The power output of the brightest LEDs was approximately 2.5 W/m^2 at 300 K. © 2004 American Institute of Physics. [DOI: 10.1063/1.1647271]

Beginning with the work of Ennen *et al.*,¹ study of the optical properties of III–V semiconductors doped with rare-earth (RE) elements has received considerable attention.² Due to the importance of the $1.54 \mu\text{m}$ region for optical communications, Er has been the main RE element to be investigated in these semiconductors. Since the room-temperature intensity of the light emission is strongly dependent upon the band-gap energy of the host material,³ wide band-gap semiconductors, such as III–V nitride semiconductors, appear to be excellent materials for device applications. RE-doped wide gap semiconductors offer the prospect of temperature-stable electrically pumped optical amplifiers and electroluminescent light emitters operating at wavelengths from the visible to the infrared. Er-doped light-emitting diodes (LEDs) represent a class of devices that emit light from the intra- $4f$ transitions of the Er^{3+} ions by means of electrical injection. Under forward bias, energy from electron–hole pairs can be transferred to the Er^{3+} ions leading to the excitation of the $4f$ electrons. This process likely involves an intermediate defect level in the GaN host. The Er^{3+} ions can also be directly excited by impact of hot carriers under reverse bias.⁴ This process is similar to excitation under cathodoluminescence. In both cases, the intra- $4f$ transitions of Er^{3+} ions give rise to sharp emission lines whose wavelengths are largely independent of the host material. This wavelength stability occurs because the outer $5s$ and $5p$ electron shells are filled and the inner $4f$ shell electrons are screened from interactions with the host. In wide band-gap

semiconductors, emission from the Er^{3+} ions is also very stable with respect to temperature of the host. Energy back-transfer and Auger processes are significantly reduced in such materials and luminescence from Er^{3+} ions can be observed at temperatures up to $\sim 500 \text{ K}$.^{5,6}

Qiu *et al.*⁷ demonstrated room temperature operation of an electroluminescent device (ELD) emitting at $1.54 \mu\text{m}$ based on an Er-doped GaN semiconductor film. The device consisted of a metal/*i*-GaN/*n*-GaN structure grown by chemical vapor deposition (CVD) on sapphire. The active region of the device, the *i*-GaN layer, was coimplanted with Er^+ and O^+ ions. High-field injection of electrons under reverse bias produced IR emission at $\sim 1.54 \mu\text{m}$ associated with the ${}^4I_{13/2} \rightarrow {}^4I_{15/2}$ transition of Er^{3+} ions. No Er^{3+} -related electroluminescence (EL) was observed under forward bias conditions. Steckl *et al.* achieved a variety of RE-doped GaN ELDs grown by molecular-beam epitaxy (MBE) using solid sources for Ga and the REs. Initial results were obtained with Er-doped GaN films,⁸ and subsequently extended to Pr-, Eu-, and Tm-doped films.⁹ Emission spectra from the GaN:Er ELDs displayed IR emission at $\sim 1.5 \mu\text{m}$. The spectra were measured over a temperature range from 250 to 400 K, with little change in the emission intensity spectrum. The ELDs also produced green emission peaks at ~ 537 and 558 nm , corresponding to radiative transitions from the ${}^2H_{11/2} \rightarrow {}^4I_{15/2}$ and ${}^4S_{3/2} \rightarrow {}^4I_{15/2}$ states, respectively. Using MBE methods, Ng *et al.*¹⁰ produced similar GaN:Er ELDs and observed both green and infrared emission. Morishima *et al.*¹¹ used gas-source MBE growth with a metallic source for Eu to produce metal–insulator–semiconductor di-

^{a)}Electronic mail: john.zavada@us.army.mil

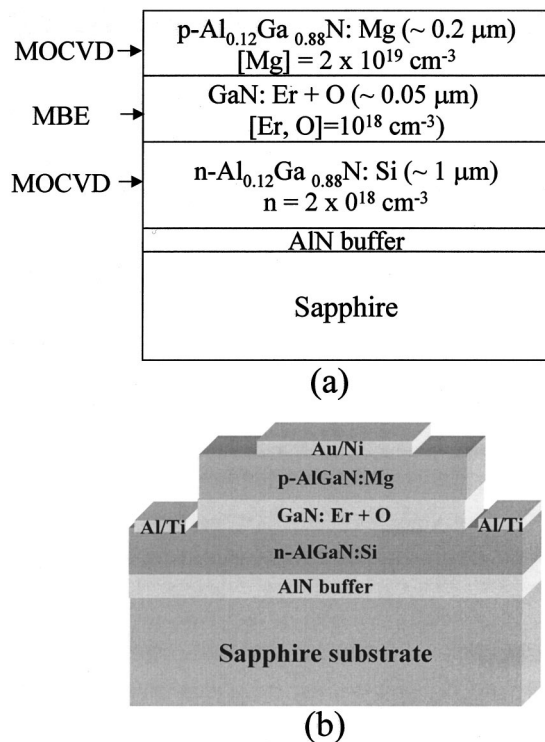


FIG. 1. (a) Schematic diagram of the III–N DH grown by MOCVD and MBE. (b) Schematic drawing of the processed LED.

odes on *n*-type Si (111) substrates. The EL spectrum from the GaN:Eu device, operated under a reverse dc bias of ~5 V, had a prominent peak at ~622 nm, corresponding to a radiative transition from the ⁵D₀ → ⁷F₂ states.

In this letter, we report on the synthesis of Er-doped III–N LEDs based on AlGaN/GaN double heterostructures (DHs) and their EL properties. The DHs were produced through a combination of metalorganic CVD (MOCVD) and MBE methods. At 300 K, these devices exhibited EL spectra characteristic of the visible and IR emission peaks of Er³⁺ ions under both forward and reverse biases. This is a demonstration of Er-doped *p*-*n* diodes formed in the III–N material system.

Synthesis of the nitride DHs involved a multistage growth process. First, AlGaN epilayers were grown by MOCVD on sapphire (0001) substrates, as described elsewhere.¹² The *n*-type layers were ~1 μm thick, with an Al content ~12%, and a Si doping ~2 × 10¹⁸ cm⁻³. The Al_{0.12}Ga_{0.88}N alloy has a band gap of ~3.75 eV. Subsequently, the GaN: Er epilayer was grown by MBE with an Er concentration of ~10¹⁸ cm⁻³.¹³ This layer was codoped with O to about the same concentration and had a thickness of 50 nm. After this stage, a second growth of AlGaN by MOCVD was performed. The top *p*-type AlGaN layer was ~200 nm thick, again with ~12% Al, and with Mg doping ~2 × 10¹⁹ cm⁻³. Room-temperature hole concentration was ~10¹⁷ cm⁻³. A schematic of the DH is shown in Fig. 1(a). Prior studies have shown that this growth sequence does not alter the photoluminescence (PL) properties of the GaN:Er epilayer.¹⁴

The fabrication procedures for Er-doped GaN LEDs were very similar to those of III–N blue and UV LEDs.^{15,16}

The devices were patterned by photolithography and inductively coupled plasma dry etching. Bilayers of Ni (20

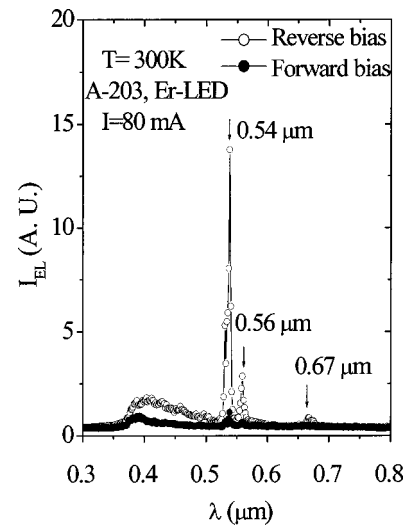


FIG. 2. Visible EL spectra for the Er-doped GaN LED with an active layer thickness of 50 nm under reverse bias (open circles) and under forward bias (solid dots).

nm)/Au (200 nm) and Al (300 nm)/Ti (20 nm) were deposited by electron-beam evaporation as *p*- and *n*-type ohmic contacts. The contacts were thermally annealed in a nitrogen ambient at 650 °C for 5 min, which was below the MBE growth temperature, and so the diffusion or intermixing of the epilayers was not expected. Figure 1(b) is a schematic diagram of the processed Er-doped III–N LED. The power output was measured from the sapphire substrate side of unpackaged bare chips by a wafer probe. Both the power output and EL spectra were measured under dc bias conditions.

Figure 2 shows the visible EL spectra, measured at 300 K, from a typical GaN:Er DH LED produced in these experiments. Measurements were made under reverse and forward biases using a current of 80 mA. The spectra display the main emission peaks of Er³⁺ ions. There is also a broad emission band from ~375 nm–500 nm, but no GaN band-edge emission was observed. While the EL spectra are simi-

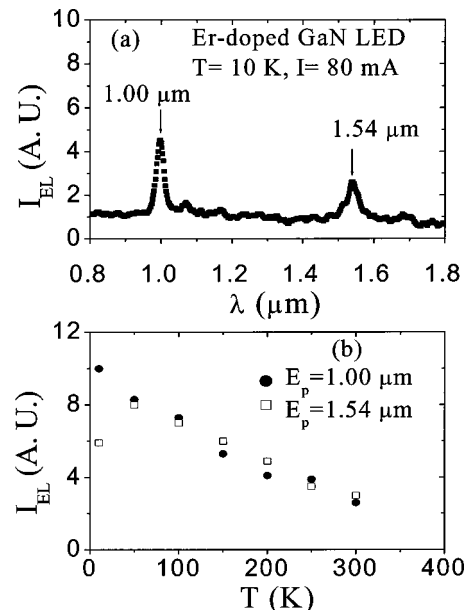


FIG. 3. (a) IR EL spectra at 10 K for the Er-doped III–N LED under reverse bias with a driving current of 80 mA. (b) The temperature dependence of the peak IR EL intensity measured at 1 μm and 1.54 μm.

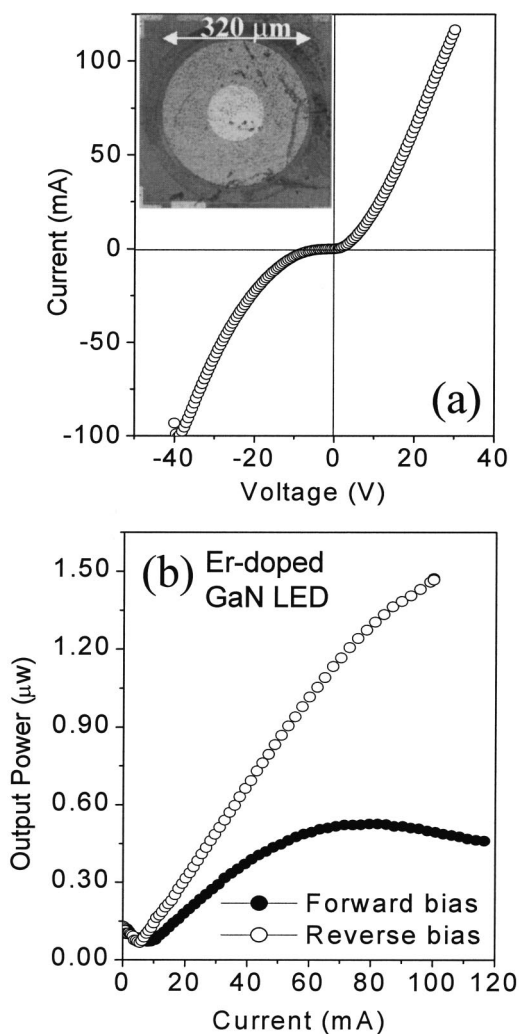


FIG. 4. (a) I - V characteristics at 300 K of the Er-doped GaN LED, the inset shows an optical micrograph of the LED; (b) Output power, integrated over the visible spectrum, under reverse bias (open circles) and under forward bias (solid dots) conditions.

lar, the emission lines are ten to fifteen times less intense with forward biasing. This is in agreement with other studies on Er-doped LEDs based on Si and SiO_x materials.^{4,17} However, using an Er-doped GaAs/InGaP DH LED, Koizumi *et al.*¹⁸ found EL only under reverse bias conditions. Apparently, under reverse bias, the Er^{3+} ions are excited by hot electrons from the junction. While the excitation mechanism under forward bias is not fully understood, it is assumed to be due to energy transfer from electron-hole pairs through an intermediate state to the Er^{3+} ions. Consequently, a DH should be more effective in confining electron-hole recombination to the region in which the Er^{3+} ions are situated.

Figure 3(a) shows the low-temperature (10 K) EL spectrum measured in the IR region under reverse bias. Two lines at 1000 nm and 1540 nm are prominent. The temperature dependence of the peak EL intensity of these IR lines is shown in Fig. 3(b). As found in previous studies, the peak EL intensity of these lines is inversely proportional to the ambient temperature.⁵ The observed EL decrease of $\sim 38\%$ from 10 K to 300 K is slightly greater than the reported PL decrease in Er-doped GaN.

In Fig. 4(a), current-voltage (I - V) characteristics are displayed for one of the DH LEDs having a diameter of 320

nm. Compared with III-N blue and UV LEDs, the rectification behavior is weaker for the Er-doped LED. The I - V plots (integrated optical power output versus forward and reverse bias) are shown in Fig. 4(b). Turn-on voltage was ~ 3.5 V for forward bias and ~ -4.5 V for reverse bias conditions. Under forward bias, the EL intensity initially increases with increasing drive current, but then saturates and reaches a maximum at ~ 70 mA. The saturation of the intensity may indicate that the concentration of optically active Er centers is a limiting factor for the EL intensity under the forward bias. Nonradiative processes may also be involved. Under reverse bias, the output power continues to increase even above 70 mA. At 100 mA, the integrated optical power output under reverse bias is nearly three times that under forward bias. Based on the dimensions of the LED, it is estimated that the maximum output power is approximately 2.5 W/m^2 at 300 K.

In summary, we have demonstrated EL emission from Er-doped GaN LEDs that were grown by MOCVD and MBE. Their EL properties were investigated under forward and reverse bias conditions. The EL spectra at room temperature indicated effective excitation of the Er^{3+} ions by current injection. The EL intensity of all emission lines was ten to fifteen times higher under reverse bias than under forward bias. The output power, integrated over the visible spectrum, of the DH LED was estimated to be $\sim 2.5 \text{ W/m}^2$ at 300 K.

The authors at KSU wish to acknowledge support by the ARO. Work done at SVT Associates was partially funded by MDA Contract No. F49620-02-C-0069, Dr. Gernot Pomrenke AFOSR, technical monitor.

¹H. Ennen, J. Schneider, G. Pomrenke, and A. Axmann, Appl. Phys. Lett. **43**, 943 (1983).

²Mater. Res. Soc. Symp. Proc., 301 (1993); *ibid.* Mater. Res. Soc. Symp. Proc., 422 (1996); Mater. Sci. Eng., B **81**, (2001).

³P. N. Favennec, H. L'Haridon, D. Moutonnet, M. Salvi, and M. Gauneau, Jpn. J. Appl. Phys., Part 2 **29**, L524 (1990).

⁴S. Lombardo, S. U. Campisano, G. N. van den Hoven, and A. Polman, J. Appl. Phys. **77**, 6504 (1995).

⁵M. Thaik, U. Hömmerich, R. N. Schwartz, R. G. Wilson, and J. M. Zavada, Appl. Phys. Lett. **71**, 2641 (1997).

⁶W. J. Choyke, R. P. Devaty, L. I. Clemen, M. Yoganathan, G. Pensl, and C. Hassler, Appl. Phys. Lett. **65**, 1668 (1994).

⁷C. H. Qiu, M. W. Leksono, J. I. Pankove, J. T. Torvik, R. J. Feuerstein, and F. Namavar, Appl. Phys. **66**, 562 (1995).

⁸A. J. Steckl and R. Birkhahn, Appl. Phys. Lett. **73**, 1700 (1998).

⁹A. J. Steckl, J. Heikenfeld, M. Garter, R. Birkhahn, and D. S. Lee, Compound Semicond. **48**, 6 (2000).

¹⁰H. M. Ng, *State-of-the-Art Program on Compound Semiconductors XXXVI and Wide Band-gap Semiconductors for Photonic and Electronic Devices and Sensors II* (Electrochemical Society, New York, 2002), Vol. 2002-3.

¹¹S. Morishima, T. Maruyama, M. Tanaka, Y. Masumoto, and K. Akimoto, Phys. Status Solidi A **176**, 113 (1999).

¹²K. B. Nam, J. Li, M. L. Nakarmi, J. Y. Lin, and H. X. Jiang, Appl. Phys. Lett. **81**, 1038 (2002).

¹³SVT Associates, Inc., Eden Prairie, MN (unpublished).

¹⁴J. M. Zavada, J. Y. Lin, H. X. Jiang, P. Chow, B. Hertog, U. Hömmerich, E. E. Nyein, and H. A. Jenkinson, Mater. Sci. Eng. B **105**, 118 (2003).

¹⁵S. X. Jin, J. Li, J. Shakya, J. Y. Lin, and H. X. Jiang, Appl. Phys. Lett. **78**, 3532 (2001).

¹⁶K. H. Kim, J. Li, S. X. Jin, J. Y. Lin, and H. X. Jiang, Appl. Phys. Lett. **83**, 566 (2003).

¹⁷S. Coffa, G. Franzo, and F. Priolo, Mater. Res. Bull. **23**, 25 (1998).

¹⁸A. Koizumi, Y. Fujiwara, K. Inoue, A. Urakami, T. Yoshikane, and Y. Takeda, Jpn. J. Appl. Phys., Part 1 **42**, 2223 (2003).